Cardiovascular Engineering and Technology, Vol. 10, No. 2, June 2019 *(© 2019)* pp. 367–379
https://doi.org/10.1007/s13239-019-00415-4

Novel T-wave Detection Technique with Minimal Processing and RR-Interval Based Enhanced Efficiency

LAKHAN DEV SHARMA and RAMESH KUMAR SUNKARIA

Department of Electronics and Communication Engineering, Dr. B. R. Ambedkar National Institute of Technology, Jalandhar 144011, India

(Received 29 August 2018; accepted 9 April 2019; published online 16 April 2019)

Associate Editor Ajit P. Yoganathan oversaw the review of this article.

Abstract
Purpose—T-wave in electrocardiogram (ECG) is a vital wave component and has potential of diagnosing various cardiac disorders. The present work proposes a novel technique for T-wave peak detection using minimal pre-processing and simple root mean square based decision rule. *Methods*—The technique uses a two-stage median filter and a Savitzky–Golay smoothing filter for pre-processing. P-QRS-complex is removed from the filtered ECG, and T-wave is left as the most prominent wave segment, which can be detected using a root mean square based adaptive threshold. An RR-interval based T-wave peak correction strategy has been proposed which can handle the challenges of morphological variations in the T-wave, thus increases the detection accuracy. *Results*—The proposed technique has been substantiated on a standard QT-database. The detection sensitivity = 97.01%, positive predictivity = 99.61%, detection error rate = 3.36%, and accuracy = 96.66% have been achieved. *Conclusions*—A T-wave detection technique requiring minimal pre-processing and with simple decision rule has been designed. The noticeably high positive predictivity rate of the proposed technique shows its efficiency to detect T-wave peak.

Keywords—ECG, T-wave, Median filter, Savitzky–Golay filter, Root mean square, RR-interval.

INTRODUCTION

T-wave is the waveform in an electrocardiogram (ECG) representing ventricular repolarization of the heart. Out of 12 leads in ECG, a normal T-wave is usually upright in leads I, II and leads V_3 to V_6.[37] However, an inverted T-wave is normal in lead aVR. T-wave is clinically significant in diagnosis of various cardiac disorders. An inverted T-wave can be associated with left ventricular hypertrophy, myocardial ischemia, bundle branch blocks and Wolff–Parkinson–White syndrome.[29] Peaked T-wave may indicate hyperkalemia, whereas, flat T-wave may indicate coronary ischemia or hypokalemia.[37] T-wave is used in diagnosis of acute myocardial infarction.[2,24,35] Both in left and right bundle branch block repolarization sequence is effected, resulting in ST-segment depression and T-wave inversion in left lateral and right precordial leads, respectively.[37] A beat to beat variation in amplitude or shape of T-wave (T-wave alternans) is useful in identifying the patients who are at increased risk of sudden cardiac death.[10,26,28,39]

Numerous techniques are present in the literature for QRS-complex detection.[5,7,13,20,21,23,27,32,40–42] However, designing an efficient technique for T-wave peak detection is tedious due to various challenges like, overlap of P-wave and T-wave, morphological variations of T-wave, varying amplitude and heart rate variations.[8] Also, low amplitude and frequency of T-wave makes it highly prone to get corrupted by noise. Nevertheless, techniques have been proposed for T-wave peak detection, such as based on wavelet transforms,[3,4,21,40] techniques using machine learning approach,[22,30] using mathematical modeling,[6,19] and Gibbs sampler.[16,17] Wavelet based techniques depends on the selection of mother wavelet and frequency band. Machine learning based techniques requires prior learning and techniques based on mathematical modeling or Gibbs sampler are computationally complex. Challenges associated with T-wave peak detection makes it an issue that can still be worked on. A computationally simple, efficient and reliable T-wave peak detection technique needs to be developed.

Address correspondence to Lakhan Dev Sharma, Department of Electronics and Communication Engineering, Dr. B. R. Ambedkar National Institute of Technology, Jalandhar 144011, India. Electronic mail: devsharmalakhan@gmail.com

This work presents a computationally simpler T-wave peak detection technique. The proposed technique uses a root mean square based thresholding for T-wave peak detection and an RR-interval based T-wave peak correction strategy. Standard QT-Database[9,14] has been used for validation of the proposed technique, which is a benchmark for the ECG waveform detection techniques.

DATABASE

QT-Database was designed to challenge the algorithms detecting various waveforms and waveform boundaries in the ECG. QT-database is a collection of 105 real-world morphologically varying ECG from subjects suffering from various cardiac arrhythmias. To construct the QT-database, records were chosen primarily from among standard existing ECG databases, including the MIT-BIH Arrhythmia Database,[25] the European Society of Cardiology ST-T Database,[36] the MIT-BIH Supraventricular Arrhythmia Database,[12] Sudden Cardiac Death Holter Database,[11] the MIT-BIH ST Change Database,[1] and the MIT-BIH Normal Sinus Rhythm Database.[9] All records of QT-Database are publicly available at sampling frequency of 250 Hz. In QT-Database, reference annotations for waveforms and waveform boundaries of the ECG records have been provided which can be used in developing techniques for their automated detection.

PROPOSED METHODOLOGY

This section describes the underlying methodology for T-wave peak detection in details. After pre-processing, the QRS-complex is detected and removed, leaving T-wave as the most prominent wave. From the QRS-removed ECG signal T-wave peak is detected. Flow diagram of the proposed technique is presented in Fig. 1.

Pre-processing

The raw ECG signal is passed through a two-stage median filter to remove the baseline wander followed by a Savitzky-Golay (SG) smoothing filter. Window width of the two stages of median filter and SG filter's order and frame size is selected as described in Refs. 32–34. Let, the ECG signal after this pre-processing stage be $x[n]$. A raw ECG signal is shown in Fig. 2, its baseline wander removed form is shown in Fig. 3 and the final signal out of pre-processing stage comes out to be as shown in Fig. 4, after passing it through the

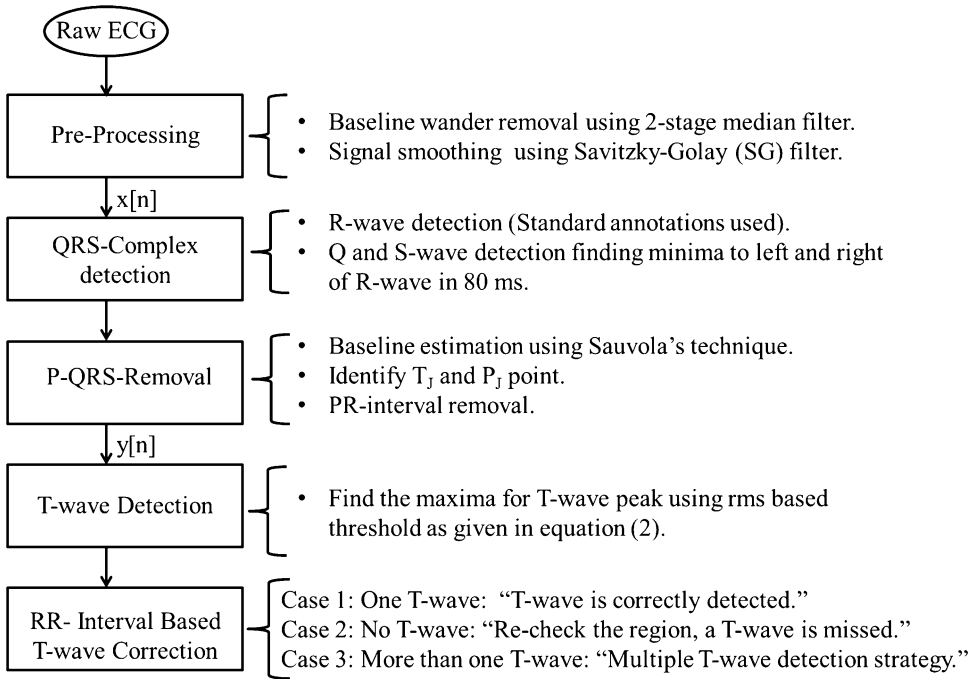

FIGURE 1. Process flow diagram.

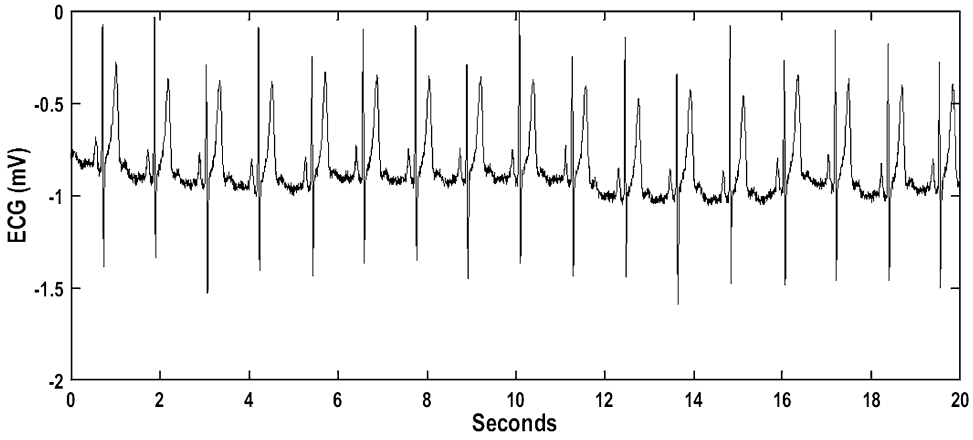

FIGURE 2. Raw ECG.

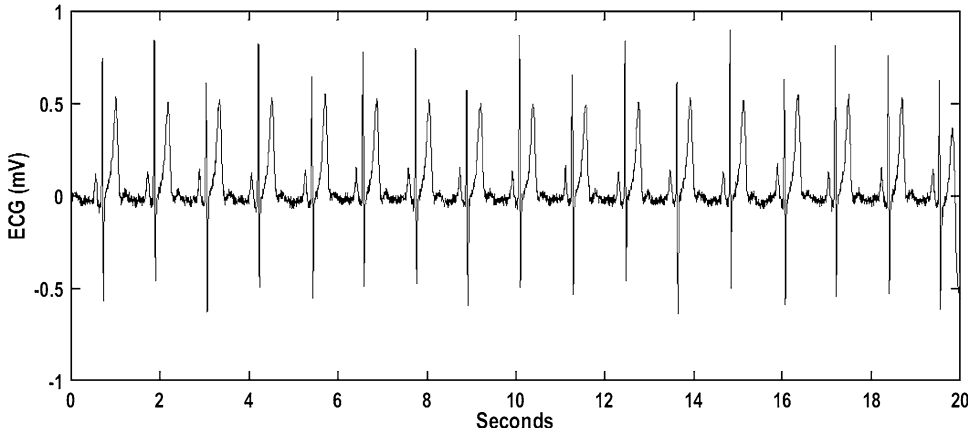

FIGURE 3. Baseline wander removed ECG.

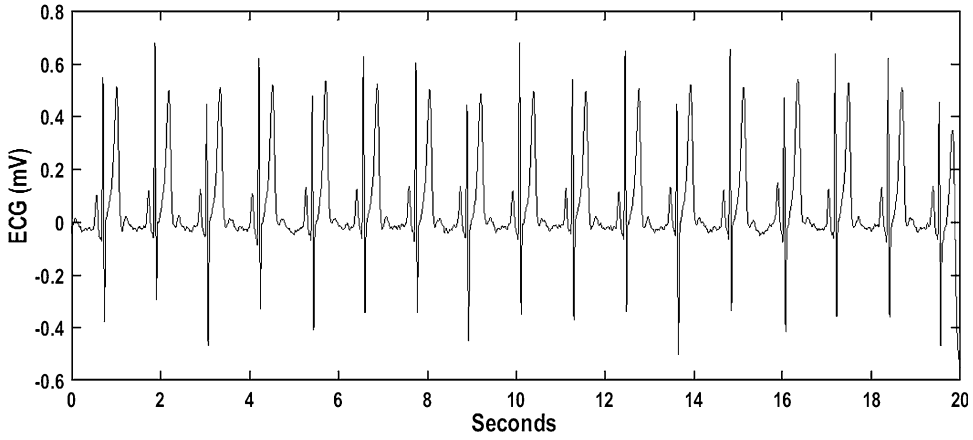

FIGURE 4. Baseline wander removed and SG-filtered ECG, $x[n]$.

SG smoothing filter. To visualize the time delay associated during pre-processing stage, a 2 s ECG signal smoothen out using the pre-processing stage is shown in Fig. 5 overlapped over the corresponding raw ECG section. Figure shows, location of the T-waves peaks in filtered ECG signal is same as that of raw ECG signal.

QRS-Complex Detection

QRS-complex is the most prominent wave in ECG signal, so it needs to be detected and removed from the signal, so that the T-wave remains as the most prominent wave in the resulting signal. QRS-complex

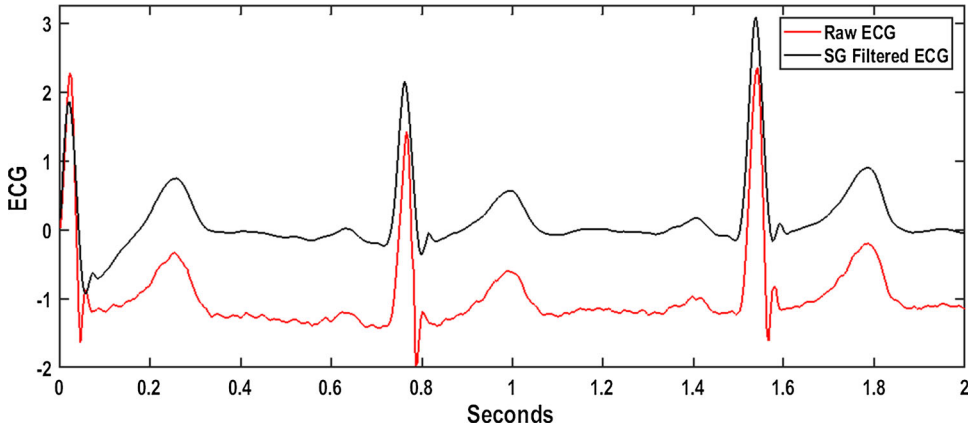

FIGURE 5. Raw ECG overlapped on its SG-filtered form.

detection has been already a highly explored area and variety of techniques are present for the task. However, in this work annotation of R-wave provided in the QT-database has been used and QRS-complex detection has been considered as a well resolved issue. Q-wave and S-wave can be determined by searching for minima on the left and right of each positive R-wave within 80 ms.

P-QRS-Complex Removal

Other than T-wave, P-wave and QRS-complex are two distinguished waveforms in the ECG. To remove P-QRS-complex from the filtered ECG $x[n]$, vital markers needs to be identified and a substitute for the removed P-QRS-complex need to be estimated.

Baseline Estimation

This technique requires to estimate the baseline, which has to be used as a substitute for the removed P-QRS-complex and to distinguish between upward and inverted T-wave. Baseline is identified using Sauvola's technique been used in image binarization process.[31] The strong potential of Sauvola's binarization method based threshold to identify the baseline has been shown in our previous work.[32]

$$B = \mu[1 + k(\sigma/\sigma_{\max} - 1)] \quad (1)$$

In Eq. (1), B is the estimated baseline, μ is mean and σ is standard deviation of $x[n]$ and $\sigma_{\max}$ is maximum standard deviation around mean. Parameter k is selected to be as in Ref. 32.

Identifying T_J and P_J Point

To completely remove the QRS-complex two points: T_J and P_J points, need to be identified. T_J point is the point after S-wave which is nearest to the estimated baseline (B). Similarly, P_J-point is the point before Q-wave which is nearest to B. In the proposed technique, the ECG segment from P_J point to T_J point has been replaced by B to completely remove the QRS-complex. Filtered ECG signal $x[n]$ with its required vital markers like baseline (B), R-wave, Q-wave, S-wave, T_J point, and P_J point is shown in Fig. 6.

PR-Interval Removal

P-wave is the most prominent wave after QRS-complex and T-wave. In some cases the amplitude of P-wave may be more than T-wave, which may result in false positive detections. Normal range of RR-interval is 0.6–1.2 s and normal range of PR-interval is 120–200 ms. To overcome the chances of false positive detection due to P-wave, $1/5\times$ (average RR-interval of the ECG) samples before the previously identified P_J point is replaced by B.

The above mentioned steps for P-QRS-complex removal is dependent on RR-interval and width of QRS-complex. Thus, the proposed technique is adaptive to the morphological variations. This P-QRS-complex removed ECG signal is denoted by $y[n]$. A section of filtered ECG signal $x[n]$ from the subject 'sel116', after pre-processing step is shown in Fig. 7a. The P-QRS-complex removed ECG signal $y[n]$ of the signal in Fig. 7a is shown in Fig. 7b. It can be observed from Fig. 7b, T-wave is left as most prominent wave in $y[n]$. As per the literatures, a normal U-wave amplitude rarely exceeds 0.2 mV; normal U-wave height is less than one-quarter that of the T-wave.[38] Hence, in the proposed technique after P-QRS-complex removal T-wave is considered to be left as most prominent wave.

T-wave Detection

The proposed technique is based on root mean square of the P-QRS-complex removed ECG signal ($y[n]$). To locate the T-wave region, following threshold is used:

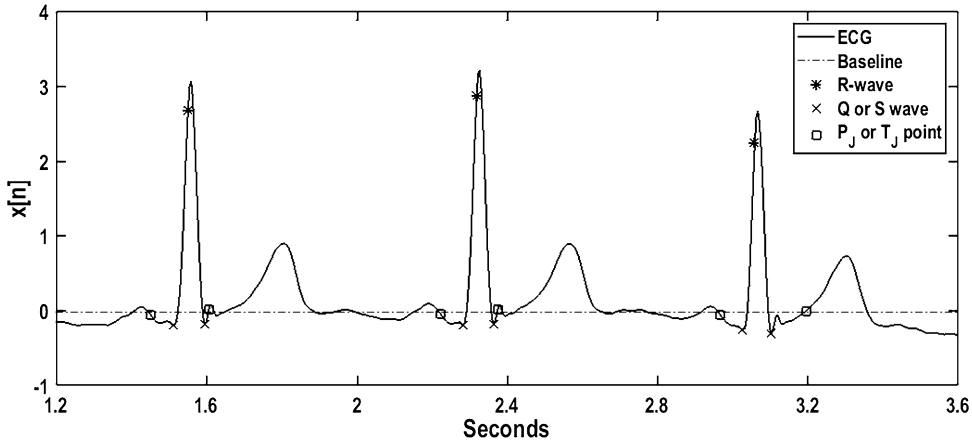

FIGURE 6. *x[n]* with baseline (B), R-wave, Q-wave, S-wave, T_J point, and P_J point marked.

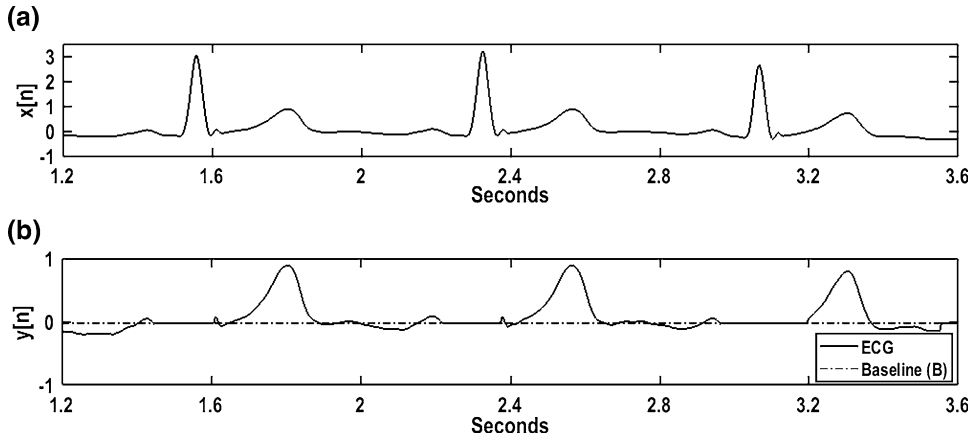

FIGURE 7. (a) Filtered ECG *x[n]*, (b) P-QRS-complex removed ECG signal *y[n]*.

$$\text{T-wave regions} = \begin{cases} \text{Upward T-wave region} & : y[n] \geq [B + y_{\text{rms}}] \\ \text{Inverted T-wave region} & : y[n] \leq [B - y_{\text{rms}}] \end{cases} \quad (2)$$

In Eq. (2), y_{rms} is root mean square value of $y[n]$. The exact location of T-wave peak is above $[B + y_{\text{rms}}]$ in case of upward T-wave region and it is the maxima of the selected region. Similarly, T-wave peak for inverted T-wave is minima of the selected region. In Fig. 8a, $y[n]$ and its estimated baseline (B) and y_{rms} based thresholds are shown. The ECG signal $x[n]$ with its detected T-wave peak is shown in Fig. 8b.

RR-Interval Based T-wave Correction

There are more complications involved in T-wave peak detection than QRS-complex detection due to variety of abnormal T-wave possibilities, like, peaked T-wave, inverted T-wave, biphasic T-wave , and 'camel hump' T-wave. An RR-interval based correction strategy has been formulated which can resolve all these abnormal T-waves and reduce the false positive and false negative cases. In the proposed methodology, the number of T-wave peaks detected between two QRS-complexes are counted and a decision is made according to the following possibilities.

One T-wave

A normal ECG has one T-wave peak between two QRS-complex. So, if the number of T-wave peak between two QRS-complex is found to be one, it is considered to be a correct detection and no further processing is needed for that T-wave location.

No T-wave

If no T-wave peak is detected between two QRS-complex, this means amplitude of the T-wave between those QRS-complexes could not cross the over all threshold, calculated using Eq. (2) and the full ECG segment. To locate that missed T-wave peak, a new local threshold has been calculated based on the section of $y[n]$ between those two QRS-complexes. The new threshold is calculated based on Eq. (2), this time

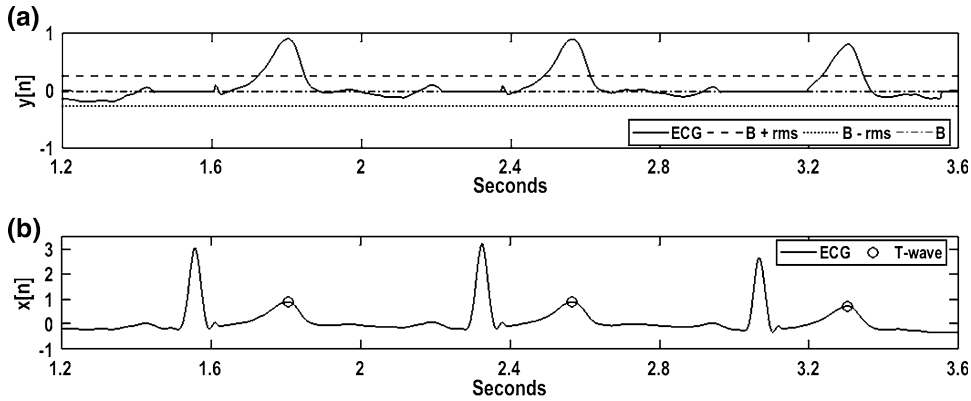

FIG. 8. 'sel116' (MLII): (a) *y*[*n*] with baseline (B) and *rms* based thresholds, (b) *x*[*n*] with detected T-wave

y_{rms} of the section of $y[n]$ between those two QRS-complexes is used and B is fixed as before. This novel strategy lowers the local threshold and makes the detection of the missed T-wave peak possible. Also, as this new threshold is dependent on that specific section of ECG this makes the proposed technique adaptive to the change in morphology of ECG.

Multiple T-wave

In the case, if more than one T-wave peak is identified between two QRS-complex then following strategy is adopted for multiple T-wave peak detection.

1. In case if two peaks are identified and they are on the same side of B, ie. both upward or both inverted then maximum of both is selected as the T-wave peak. This overcomes the problem of 'camel hump' T-wave.
2. In case if two peaks are identified, out of which first is below B and second is above B then first is discarded.
3. In case if two peaks are identified, out of which first is above B and second is below B, ie. an upward T-wave is preceded by an inverted T-wave, this is a case of biphasic T-wave. In this case both the points are kept and the T-wave is identified as a biphasic T-wave.
4. In case more than two T-wave peaks appear, then farthest of all from B is selected as T-wave peak.

RESULTS

The proposed technique uses T-wave annotation provided in the QT-database for validation purpose. Channel I of 60 records from this database have been used, detailed results for which are shown in Table 1. The performance of the proposed technique is evaluated using detection sensitivity (Se%), positive predictivity rate (+P%), detection error rate (DER%), and accuracy (Ac%). Se% is given as in Eq. (3).

$$Se\% = \frac{TP}{TP + FN} * 100 \tag{3}$$

Here, true positive (TP) is the number of correct T-wave peak predictions. FN is false negative, where the proposed technique predicts there is no T-wave peak but a real T-wave peak exists in that location. +P% can be expressed as in Eq. (4).

$$+\mathrm{P}\% = \frac{\mathrm{TP}}{\mathrm{TP} + \mathrm{FP}} * 100 \tag{4}$$

Here, FP is false positive prediction. It is the location where the proposed technique predicts a T-wave peak but there is no T-wave peak in real. DER% is defined as in Eq. (5).

$$\mathrm{DER}\% = \frac{\mathrm{FN} + \mathrm{FP}}{\mathrm{TP} + \mathrm{FN}} * 100 \tag{5}$$

Ac% of the proposed technique is calculated by Eq. (6).

$$\mathrm{Ac}\% = \frac{\mathrm{TP}}{\mathrm{TP} + \mathrm{FN} + \mathrm{FP}} * 100 \tag{6}$$

As observed from Table 1, the proposed technique has noticeable high +P% = 99.61%. The high value of +P% has been achieved due to less number of false positive detections, resulting because of the proposed RR-interval based T-wave peak correction strategy. A satisfactory value of Se% = 97.01 has been achieved. This value can be further improved by working on a definition to better characterize a biphasic T-wave. As most of the false negative is due to the biphasic T-wave, where during inverted phase it could not cross the set threshold.

TABLE 1. Performance evaluation of the proposed technique on QT-database.

ECG record	Total beats	TP	FN	FP	Se%	+P%	DER%	Ac%
sele0704	1786	1691	95	0	94.68	100.00	5.32	94.68
sele0612	769	767	2	0	99.74	100.00	0.26	99.74
sele0609	1269	1197	72	0	94.33	100.00	5.67	94.33
sele0606	1453	1442	11	0	99.24	100.00	0.76	99.24
sele0604	1035	1029	6	0	99.42	100.00	0.58	99.42
sele0603	1620	1530	90	1	94.44	99.93	5.62	94.39
sele0509	1025	1025	0	3	100.00	99.71	0.29	99.71
sele0411	1292	1201	91	0	92.96	100.00	7.04	92.96
sele0409	1782	1781	1	1	99.94	99.94	0.11	99.89
sele0406	975	960	15	0	98.46	100.00	1.54	98.46
sele0211	1593	1574	19	0	98.81	100.00	1.19	98.81
sele0210	1080	1061	19	0	98.24	100.00	1.76	98.24
sele0170	900	895	5	0	99.44	100.00	0.56	99.44
sele0166	923	833	90	1	90.25	99.88	9.86	90.15
sele0136	855	818	37	3	95.67	99.63	4.68	95.34
sele0133	873	825	48	16	94.50	98.10	7.33	92.80
sele0124	1181	1119	62	2	94.75	99.82	5.42	94.59
sele0122	1414	1412	2	0	99.86	100.00	0.14	99.86
sele0121	1431	1431	0	1	100.00	99.93	0.07	99.93
sele0110	906	872	34	0	96.25	100.00	3.75	96.25
sele0107	845	820	25	0	97.04	100.00	2.96	97.04
sele0106	879	858	21	36	97.61	95.97	6.48	93.77
sel873	865	859	6	0	99.31	100.00	0.69	99.31
sel872	1026	989	37	0	96.39	100.00	3.61	96.39
sel847	814	801	13	0	98.40	100.00	1.60	98.40
sel840	1306	1180	126	0	90.35	100.00	9.65	90.35
sel821	1558	1558	0	1	100.00	99.94	0.06	99.94
sel803	1037	1027	10	0	99.04	100.00	0.96	99.04
sel44	1476	1451	25	25	98.31	98.31	3.39	96.67
sel38	1559	1559	0	0	100.00	100.00	0.00	100.00
sel36	1075	979	90	15	91.58	98.49	9.82	90.31
sel34	907	907	0	29	100.00	96.90	3.20	96.90
sel33	525	525	0	14	100.00	97.40	2.67	97.40
sel32	1228	1193	35	4	97.15	99.67	3.18	96.83
sel30	1152	1031	115	0	89.97	100.00	10.03	89.97
sel308	1306	1293	13	1	99.00	99.92	1.07	98.93
sel307	859	850	9	1	98.95	99.88	1.16	98.84
sel306	1045	1038	7	0	99.33	100.00	0.67	99.33
sel302	1513	1499	14	0	99.07	100.00	0.93	99.07
sel233	1538	1530	8	0	99.48	100.00	0.52	99.48
sel232	947	886	61	2	93.56	99.77	6.65	93.36
sel221	1410	1292	118	3	91.63	99.77	8.58	91.44
sel17453	1143	1044	99	0	91.34	100.00	8.66	91.34
sel17152	1723	1626	97	0	94.37	100.00	5.63	94.37
sel16795	759	757	2	1	99.74	99.87	0.40	99.61
sel16786	925	922	3	0	99.68	100.00	0.32	99.68
sel16773	1064	1005	59	1	94.45	99.90	5.64	94.37
sel16539	931	916	15	2	98.39	99.78	1.83	98.18
sel16483	1084	1083	1	1	99.91	99.91	0.18	99.82
sel16420	1175	1063	112	0	90.47	100.00	9.53	90.47
sel16273	1112	1109	3	0	99.73	100.00	0.27	99.73
sel16272	849	848	1	0	99.88	100.00	0.12	99.88
sel16265	1032	1029	3	0	99.71	100.00	0.29	99.71
sel15814	1024	1024	0	9	100.00	99.13	0.88	99.13
sel14172	732	650	82	26	88.80	96.15	14.75	85.75
sel123	771	750	21	2	97.28	99.73	2.98	97.02
sel117	765	764	1	0	99.87	100.00	0.13	99.87
sel116	1188	1185	3	0	99.75	100.00	0.25	99.75
sel114	963	871	92	5	90.45	99.43	10.07	89.98
sel103	1048	1046	2	0	99.81	100.00	0.19	99.81

TABLE 1. Continued

ECG record	Total beats	TP	FN	FP	Se%	+P%	DER%	Ac%
Overall result	67,320	65,292	2028	206	97.01	99.61	3.36	96.66

TP true positive , *FN* false negative, *FP* false positive, *Se*% sensitivity, +*P*% positive predictivity rate, *DER*% detection error rate, and *Ac*% accuracy.

TABLE 2. Comparison of the proposed technique from state-of-art algorithms.

Techniques	Se%	+P%	References
Bayesian approach and Gibbs sampler	99.81	98.97	17
Support vector machine	96.83*	96.90*	22
Continuous wavelet transform	99.17	84.46	40
Instantaneous P- and T-wave detection	89.40	80.00	15
Proposed technique	97.01	99.61	–

*Calculated from the data given in the paper.

The proposed technique has been compared with the state-of-art algorithms in Table 2. The + P% of the proposed technique is considerably higher than the present algorithms.[15,17,22,40] Whereas, Se% of the proposed technique is comparable to the heuristic techniques based on machine learning like support vector machine.[15,22]

DISCUSSION

The proposed technique can detect biphasic T-wave peaks. An example for detection of biphasic T-wave peaks is shown in Fig. 9. In Fig. 9a, $y[n]$ with its baseline and y_{rms} based thresholds are shown. In Fig. 9b, the signal $x[n]$ with its detected T-wave peaks are shown. The ability of the proposed technique to detect biphasic T-wave peaks are evident from Fig. 9.

If no T-wave peak is detected between two QRS-complexes, then the region between them is processed again and the missed T-wave peak is detected. As shown in Fig. 10a, the 3rd T-wave could not cross the upper threshold to get detected. However, it gets detected due to the proposed RR-interval based T-wave peak correction strategy.

The proposed technique can work even in the case of inverted QRS-complex, example of which is shown in Fig. 11.

Figures 12 and 13 are examples for successful detection of inverted T-wave peaks. In Fig. 12 QRS-complex in inverted and in Fig. 13 QRS-complex is upward, but in both the cases the proposed technique can detect inverted T-wave peaks successfully.

Ability of the proposed technique to work for peaked T-wave is shown in Fig. 14. The proposed technique successfully works in the case when amplitude of T-wave is higher than respective QRS-complex.

Computational Time Analysis

Several factors influence the computational time of an algorithm, like processor frequency, operating system used, computational capabilities of the computer used including RAM and CPU. We have implemented our algorithm on laptop with intel core i3 2.30 GHz processor, 6 GB RAM, and 64-bit Windows 10 operating system. MATLAB R2017a has been used for implementation of this algorithm. For 15 s ECG signals at sampling frequency of 250 Hz from QT-database, this algorithm has shown an average computation processing time of 2.04 s. This shows computational efficiency of the proposed technique compared to the state-of-art techniques, like P-QRS-T detection proposed by Maxime Yochuma et al. and Li et al., which takes 48.6 and 60.0 s respectively for 10 s ECG signal.[18,40]

HIGHLIGHTS

The achievements of this work needs to be highlighted are as follows:

– The proposed technique works with minimum pre-processing requirements and on simple decision logic.

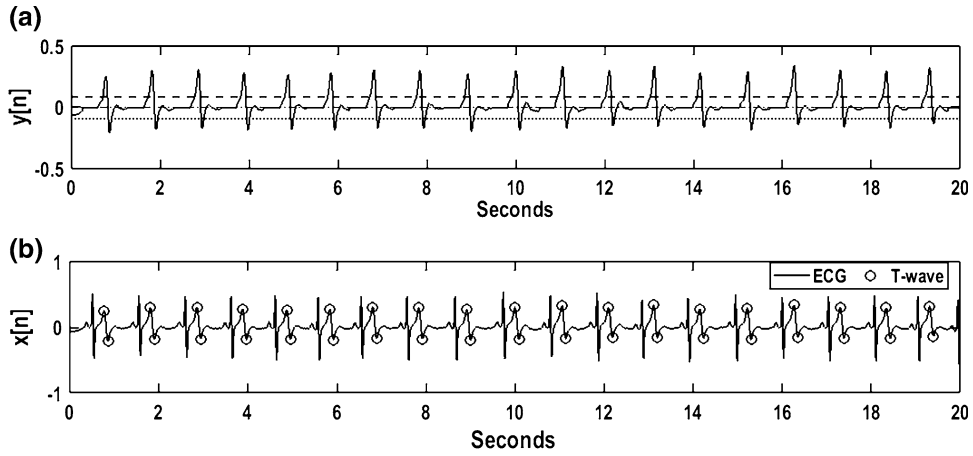

FIGURE 9. 'sele0603m' (CM5): (a) $y[n]$ with baseline (B) and y_{rms}rms based thresholds, (b) $x[n]$ with detected T-wave.

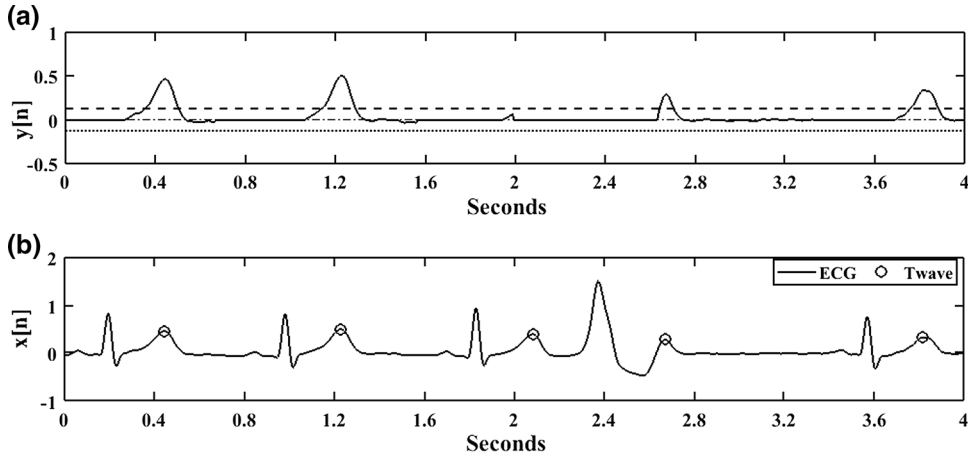

FIGURE 10. 'sele0411m' (CM5): (a) $y[n]$ with baseline (B) and y_{rms} based thresholds, (b) $x[n]$ with detected T-wave.

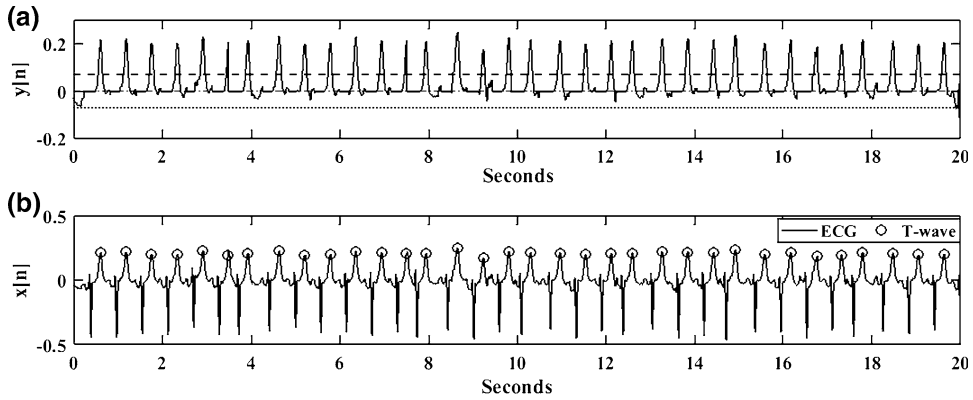

FIGURE 11. 'sel821m' (ECG1): (a) $y[n]$ with baseline (B) and y_{rms} based thresholds, (b) $x[n]$ with detected T-wave.

– In this work, an RR-interval based T-wave peak correction strategy to deal with morphological variations in the T-waves has been proposed.
– The proposed technique has been validated on a standard QT-database

LIMITATION AND FUTURE SCOPE

The proposed technique has following limitations which can be worked on, in future research works:

– The proposed technique can detect T-waves peaks. However, detecting T-wave boundaries

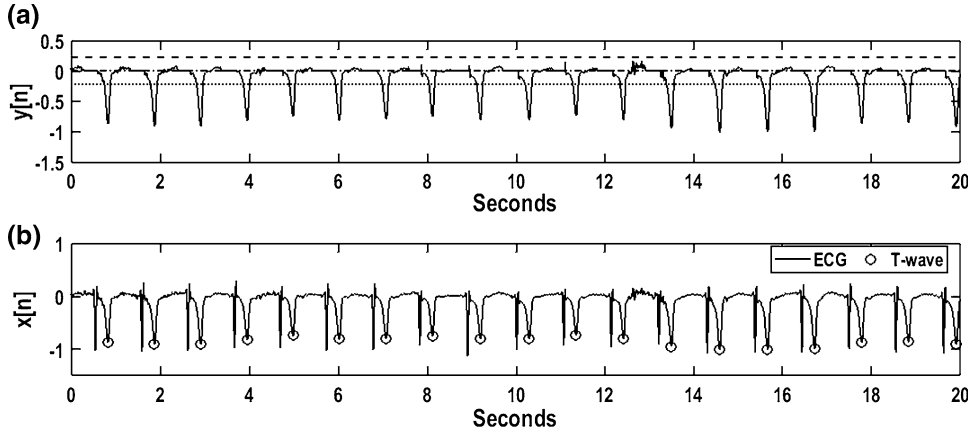

FIGURE 12. 'sele0107'(D3): (a) $y[n]$ with baseline (B) and y_{rms} based thresholds, (b) $x[n]$ with detected T-wave.

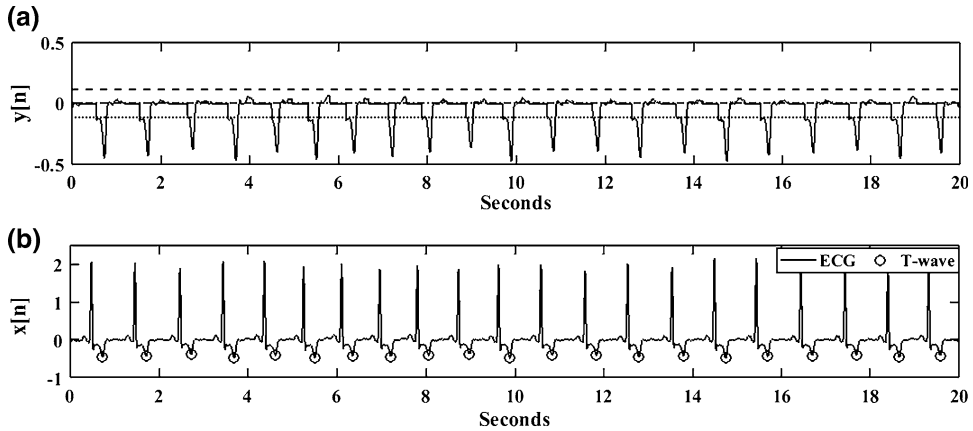

FIGURE 13. 'sel306m' (ECG1): (a) $y[n]$ with baseline (B) and y_{rms} based thresholds, (b) $x[n]$ with detected T-wave.

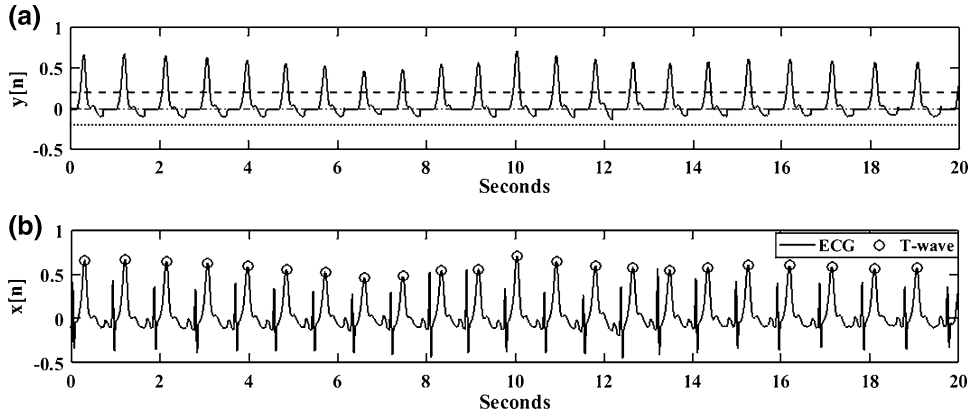

FIGURE 14. 'sele0604m' : (a) $y[n]$ with baseline (B) and y_{rms} based thresholds, (b) $x[n]$ with detected T-wave.

(i.e. T-wave on-set and T-wave off-set) is another challenge needed to be addressed for complete delineation of the T-wave.

– The proposed technique needs to detect the R-peak locations for removal of P-QRS-complex and for its RR-interval based T-wave peak correction strategy.
– Since the proposed technique uses R-peak locations as a reference for its RR-interval based T-wave peak correction strategy, so if an

TABLE 3. Limitation analysis of the proposed technique compared to state-of-art algorithms

Author	Year	QRS detection	References
Cesari *et al.*	2017	Required	3
Leutheuser *et al.*	2016	Required	15
Yochuma *et al.*	2016	Required	40
Elgendi *et al.*	2015	Required	8
Lin e*et al.*	2014	Required	16
Saini *et al.*	2014	Required	30
Madeiro*et al.*	2013	Required	19
Lin *et al.*	2010	Required	17
Mehta *et al.*	2009	Required	22
Proposed technique	–	Required	–

R-wave is missing in the QRS-complex then its T-wave may also get undetected.

Since the proposed technique requires accurate detection of QRS complex for its working, we have done a comparative limitation analysis in Table 3 with respect to the present state-of-art algorithms. QRS-complex is the most prominent wave in the ECG segment and it works as a reference for detection of other wave components, so most of the T-wave detection technique requires detection of QRS-complex in its preprocessing stage.

CONCLUSION

In the present work, a novel T-wave peak detection technique has been proposed using minimal pre-processing and simple decision rules. The proposed technique used a two-stage median filter for baseline wander removal and an SG-filter for signal smoothing. T-wave peak is detected from the P-QRS-complex removed ECG signal. An RR-interval based T-wave peak correction strategy has been proposed which enables the technique to work even in cases of morphological variations in the T-wave. The proposed technique has been validated on a standard QT-database and Se% = 97.01%, +P% = 99.61%, DER% = 3.36%, and Ac% = 96.66% have been achieved. The proposed technique can work efficiently even in the presence of morphological variations in QRS-complex or T-wave.

ACKNOWLEDGMENTS

Authors are thankful to the Ministry of Human Resource Development, Government of India for providing the financial assistance. This work has been done at Medical Imaging and Computational Modeling of Physiological System Research Laboratory at Department of Electronics and Communication Engineering of Dr. B. R. Ambedkar National Institute of Technology, Jalandhar, India.

CONFLICT OF INTEREST

Authors declare that they have no conflict of interest.

HUMAN STUDIES/INFORMED CONSENT

This work uses freely available standard QT-Database for validation of the proposed technique. No human studies were carried out by the authors for this article.

RESEARCH INVOLVING ANIMAL RIGHTS

No animal studies were carried out by the authors for this article.

REFERENCES

[1]Albrecht, P. ST segment characterization for long term automated ECG analysis, Ph.D. thesis, Massachusetts Institute of Technology, Department of Electrical Engineering, 1983.
[2]Arif, M., I. A. Malagore, and F. A. Afsar. Detection and localization of myocardial infarction using k-nearest neighbor classifier. *J. Med. Syst*. 36(1):279–289, 2012.
[3]Cesari, M., J. Mehlsen, A.-B. Mehlsen, and H. B. D. Sorensen. A new wavelet-based ECG delineator for the evaluation of the ventricular innervation. *IEEE J. Transl. Eng. Health Med*. 5:1–15, 2017.
[4]Chen, P.-C., S. Lee, and C.-D. Kuo. Delineation of T-wave in ECG by wavelet transform using multiscale differential operator. *IEEE Trans. Biomed. Eng*. 53(7):1429–1433, 2006.
[5]Deepu, C. and Y. Lian. A joint QRS detection and data compression scheme for wearable sensors. *IEEE Trans. Biomed. Eng*. 62:165–175, 2014.
[6]do Vale Madeiro, J. P., E. M. B. E. dos Santos, P. C. Cortez, J. H. da Silva Felix, and F. S. Schlindwein. Evaluating gaussian and rayleigh-based mathematical models for T and P-waves in ECG. *IEEE Latin Am. Trans*. 15(5):843–853, 2017.
[7]Dohare, A. K., V. Kumar, and R. Kumar. An efficient new method for the detection of QRS in electrocardiogram. *Comput. Electr. Eng*. 40(5):1717–1730, 2014.
[8]Elgendi, M., B. Eskofier, D. Abbott. Fast T wave detection calibrated by clinical knowledge with annotation of P and T waves. *Sensors* 15(7):17693–17714, 2015.
[9] Goldberger A., L. Amaral, L. Glass, J. Hausdorff, P. Ivanov, R. Mark, J. Mietus, G. Moody, C. K. Peng, and H. Stanley. PhysioBank, PhysioToolkit, PhysioNet, com-

ponents of a new research resource for complex physiologic signals. *Circulation* 101(23):e215–e220, 2000.
[10]Goya-Esteban, R., O. Barquero-Perez, M. Blanco-Velasco, A. Caamano-Fernandez, A. Garcia-Alberola, and J. L. Rojo-Alvarez. Nonparametric signal processing validation in T-wave alternans detection and estimation. *IEEE Trans. Biomed. Eng*. 61(4):1328–1338, 2014.
[11]Greenwald, S. D. The development and analysis of a ventricular fibrillation detector, Ph.D. thesis, Massachusetts Institute of Technology, 1986.
[12]Greenwald, S. D., R. S. Patil, and R. G. Mark. Improved detection and classification of arrhythmias in noise-corrupted electrocardiograms using contextual information. In: Proceedings of the Computers in Cardiology. IEEE, pp. 461–464, 1990.
[13]Khaled, A., and B. Abdelhak. Sigmoidal radial basis function ANN for QRS complex detection. *Neurocomputing* 145:438–450, 2014.
[14]Laguna, P., R. G. Mark, A. Goldberg, and G. B. Moody. A database for evaluation of algorithms for measurement of QT and other waveform intervals in the ECG. In: Proceedings of the Computers in Cardiology, IEEE, pp. 673–676, 1997.
[15]Leutheuser, H., S. Gradl, L. Anneken, M. Arnold, N. Lang, S. Achenbach, and B. M. Eskofier. Instantaneous P-and T-wave detection: assessment of three ECG fuducial points detection algorithms, In: 13th International Conference on Wearable and Implantable Body Sensor Networks (BSN). IEEE, pp. 329–334, 2016.
[16]Lin, C., G. Kail, A. Giremus, C. Mailhes, J.-Y. Tourneret, and F. Hlawatsch. Sequential beat-to-beat P and T wave delineation and waveform estimation in ECG signals: Block gibbs sampler and marginalized particle filter. *Signal Process*. 104:174–187, 2014.
[17]Lin, C., C. Mailhes, and J.-Y. Tourneret. P-and T-wave delineation in ECG signals using a bayesian approach and a partially collapsed gibbs sampler. *IEEE Trans. Biomed. Eng*. 57(12):2840–2849, 2010.
[18]Li, C., C. Zheng, and C. Tai. Detection of ecg characteristic points using wavelet transforms. *IEEE Trans. Biomed. Eng*. 42(1):21–28, 1995.
[19]Madeiro, J. P., W. B. Nicolson, P. C. Cortez, J. A. Marques, C. R. Vazquez-Seisdedos, N. Elangovan, G. A. Ng, and F. S. Schlindwein. New approach for T-wave peak detection and T-wave end location in 12-lead paced ECG signals based on a mathematical model. *Med. Eng. Phys*. 35(8):1105–1115, 2013.
[20]Manikandan, M. S., and K. Soman. A novel method for detecting R-peaks in electrocardiogram ECG signal. *Biomed. Signal Process. Control* 7(2):118–128, 2012.
[21]Martinez, J. P., R. Almeida, S. Olmos, A. P. Rocha, and P. Laguna. A wavelet-based ECG delineator: evaluation on standard databases. *IEEE Trans. Biomed. Eng*. 51(4):570–581, 2004.
[22]Mehta, S. S., and N. S. Lingayat. Application of support vector machine for the detection of P-and T-waves in 12-lead electrocardiogram. *Comput. Methods Prog. Biomed*. 93(1):46–60, 2009.
[23]Merino, M., I. M. Gomez, and A. J. Molina. Envelopment filter and K-means for the detection of QRS waveforms in electrocardiogram. *Med. Eng. Phys*. 37(6):605–609, 2015.
[24]Mitra, S., M. Mitra, and B. B. Chaudhuri. A rough-set-based inference engine for ECG classification. *IEEE Trans. Instrum. Meas*. 55(6):2198–2206, 2006.
[25]Moody, G. B. , and R. G. Mark. The MIT-BIH arrhythmia database on CD-ROM and software for use with it. In: Proceedings of the Computers in Cardiology. IEEE, pp. 185–188, 1990.
[26]Nemati, S., O. Abdala, V. Monasterio, S. Yim-Yeh, A. Malhotra, and G. D. Clifford. A nonparametric surrogate-based test of significance for T-wave alternans detection. *IEEE Trans. Biomed. Eng*. 58(5):1356–1364, 2011.
[27]Ning, X., and I. W. Selesnick. ECG enhancement and QRS detection based on sparse derivatives. *Biomed. Signal Process. Control* 8(6):713–723, 2013.
[28]Orini, M., B. Hanson, V. Monasterio, J. P. Martinez, M. Hayward, P. Taggart, and P. Lambiase. Comparative evaluation of methodologies for T-wave alternans mapping in electrograms. *IEEE Trans. Biomed. Eng*. 61(2):308–316, 2014.
[29]Pillarisetti, J., and K. Gupta. Giant inverted T waves in the emergency department: case report and review of differential diagnoses. *J. Electrocardiol*. 43(1):40–42, 2010.
[30]Saini, I., D. Singh, and A. Khosla. K-nearest neighbour-based algorithm for P-and T-waves detection and delineation. *J. Med. Eng. Technol*. 38(3):115–124, 2014.
[31]Shafait, F., D. Keysers, and T. M. Breuel. Efficient implementation of local adaptive thresholding techniques using integral images. In: Proceedings of the Electronic Imaging 2008, International Society for Optics and Photonics, pp. 681510–681510, 2008.
[32]Sharma, L. D., and R. K. Sunkaria. A robust QRS detection using novel pre-processing techniques and kurtosis based enhanced efficiency. *Measurement* 87:194–204, 2016.
[33]Sharma, L. D., and R. K. Sunkaria. Inferior myocardial infarction detection using stationary wavelet transform and machine learning approach. *Signal Image Video Process*. 12(2):199–206, 2018.
[34]Sharma, L. D. and R. K. Sunkaria. Stationary wavelet transform based technique for automated external defibrillator using optimally selected classifiers. *Measurement* 125:29–36, 2018.
[35]Shenthar, J., S. Deora, M. Rai, and C. N. Manjunath. Prolonged T peak-end and T peak- end/QT ratio as predictors of malignant ventricular arrhythmias in the acute phase of ST- segment elevation myocardial infarction: a prospective case-control study. *Heart Rhythm* 12(3):484–489, 2015.
[36]Taddei, A., A. Biagini, G. Distante, M. Emdin, M. Mazzei, P. Pisani, N. Roggero, M. Varanini, R. Mark, and G. Moody, et al. The european ST-T database: development, distribution and use. In: Proceedings Computers in Cardiology. IEEE, pp. 177–180, 1990.
[37]ThalerM. S. The Only EKG Book You'll Ever Need. Philadelphia: Lippincott Williams and Wilkins, 2010.
[38]Verma, N., V. M. Figueredo, A. M. Greenspan, and G. S. Pressman. Giant U waves: an important clinical clue. *Res. Rep. Clin. Cardiol*. 2:51–55, 2011.
[39]Wan, X., Y. Li, C. Xia, M. Wu, J. Liang, and N. Wang. A T-wave alternans assessment method based on least squares curve fitting technique. *Measurement* 86:93–100, 2016.

[40]Yochum, M., C. Renaud, and S. Jacquir. Automatic detection of P, QRS and T patterns in 12 leads ECG signal based on CWT. *Biomed. Signal Process. Control* 25:46–52, 2016.

[41]Zidelmal, Z., A. Amirou, M. Adnane, and A. Belouchrani. Qrs detection based on wavelet coefficients. *Comput. Methods Prog. Biomed.* 107(3):490–496, 2012.

[42]Zidelmal, Z., A. Amirou, D. Ould-Abdeslam, A. Moukadem, and A. Dieterlen. QRS detection using S-transform and shannon energy. *Comput. Methods Prog. Biomed.* 116(1):1–9, 2014.